Insulin growth factor signaling mediates neuron-like differentiation of adipose tissue-derived stem cells

Hongxiu Ning, **Guiting Lin**, **Thomas Fandel**, **Lia Banie**, **Tom F. Lue**, and **Ching-Shwun Lin**
Knuppe Molecular Urology Laboratory Department of Urology, School of Medicine, University of California San Francisco, CA 94143-0738, USA Tel: 11 415 476 3800 Fax: 11 415 476 3803

Abstract

Our previous study showed that adipose tissue-derived stem cells (ADSC) could be induced by isobutylmethylxanthine (IBMX) to differentiate into neuron-like cells. In the present study, ADSC were treated with IBMX in the presence or in the absence of each of eight specific inhibitors of different signaling pathways (JAK/STAT, PKA, PI3K, MEK, Wnt/Frizzled, ERK/MAPK, TGF-β, and insulin growth factor [IGF]-I). PPP, a specific inhibitor of IGF-I signaling, was the only inhibitor that showed significant inhibition of IBMX-induced ADSC neuronal differentiation, as determined by changes in cell morphology in the initial screening. Further examination by immunofluorescence staining showed that the neuronal marker, β-III-tubulin, was highly induced in IBMX-treated ADSC, and the induction was significantly suppressed by PPP. Western blotting, followed by densitometry showed that PPP suppressed IBMX-induced β-III-tubulin expression by 43%, 88%, and 84% when used to treat the cells for 1, 3, and 24 hr, respectively. Treatment of ADSC with IBMX also led to the phosphorylation of IGF-I receptor at tyrosine 1136 (Y1136), as determined by immunofluorescence staining with an antibody that reacts specifically with Y1136. This effect was also abrogated by PPP. Thus, the IBMX-induced neuron-like differentiation of ADSC is mediated by IGF signaling through the phosphorylation of IGF-IR at Y1136.

Keywords

neuron; adipose tissue-derived stem cells; differentiation; IBMX β-III-tubulin; IGF-I receptor

Introduction

Adipose tissue-derived stem cells (ADSC) are cells isolated from the stromal vascular fraction (SVF) of adipose tissues (Gronthos et al., 2001; Zuk et al., 2001). These cells also have several other names, including "adipose tissue-derived stromal cells," which was used in our previous publication (Ning et al., 2006). Now, because of the growing evidence that ADSC are bona fide adult stem cells, we decided to use the term "ADSC."

ADSC bear a strong resemblance to bone marrow stem cells (BMSC) in many aspects, including cell surface markers, gene expression profiles, and differentiation potentials (Gronthos et al., 2001; Zuk et al., 2001, 2002; De Ugarte et al., 2003; Lee et al., 2004; Case et al., 2005; Dicker et al., 2005; Strem et al., 2005; Wagner et al., 2005; Liu et al., 2007; Yoshimura et al., 2007). Unlike BMSC, however, the source of ADSC is a tissue that can be obtained in large quantities and with low risks (Housman et al., 2002). Furthermore, on a per gram basis, adipose tissue also yields far more stem cells than the bone marrow (5,000

versus 100–1,000) (Strem et al., 2005). Therefore, it is reasonable to expect that ADSC will be the preferred adult stem cells for future clinical applications.

ADSC are capable of differentiating into diverse cell types including neurons (Safford et al., 2002, 2004; Zuk et al., 2002; Ashjian et al., 2003; Kang et al., 2003, [2006]; Tholpady et al., 2003; Yang et al., 2004; Case et al., 2005; Fujimura et al., 2005; Jack et al., 2005; Guilak et al., 2006; Ning et al., 2006). We are interested in ADSC's neuronal differentiation because of our ongoing interest in finding effective treatments for urological diseases such as neurogenic erectile dysfunction and neurogenic bladder dysfunction. We have previously shown that ADSC appeared to undergo neuronal differentiation when treated with neural induction medium (NIM) or, more simply, with isobutylmethylxanthine (IBMX), which is one of the three active ingredients of NIM (Ning et al., 2006). In the present study, we extended the research to explore the molecular mechanism of IBMX-induced neuronal differentiation of ADSC. We have obtained evidence that the insulin growth factor (IGF-I) signaling pathway was involved in the process.

Materials and methods

Neuronal induction

ADSC at passages 2–5 were seeded into six-well plates or 100 mm dishes at 40%–60% confluence in Dubelco's modified Eagle's medium (DMEM). The next day, the cells were washed three times with phosphate-buffered saline (PBS) and the medium was changed to DMEM supplemented with 500 μM IBMX (Sigma-Aldrich, St. Louis, MO). The cells were then examined by HE staining, immunofluorescence staining, and/or Western blotting.

Signaling pathway screening

ADSC were seeded into six-well plates at 40%–60% confluence in DMEM. The next day, each inhibitor was added to the culture medium at a previously determined effective concentration (Table 1) (Mao et al., 2001; Laping et al., 2002; Girnita et al., 2004; Kim et al., 2005; Lin et al., 2006). One hour later, the cells were washed three times with PBS, induced with IBMX in the presence or in the absence of the same inhibitor for another hour, and examined by HE staining. The stained cells were visualized under a microscope at $\times 200$ magnification and photographed. From the photographs, a total of 1,000 cells in each treatment were scored as "+" for neuron-like morphology (condensed cell body with cellular processes) or "–" for non-neuron morphology (the original ADSC morphology).

Immunofluorescence staining

ADSC at passages 2–5 were seeded into six-well plates or 100 mm dishes at 40%–60% confluence in DMEM. The next day, neuronal induction was performed as described above in the absence or presence of 2.5 mM of PPP. The cells were then fixed with ice-cold methanol for 8 min, permeabilized with 0.05% Triton X-100 for 5 min, and blocked with 5% normal horse serum in PBS for 1 hr at room temperature. The cells were then incubated with an anti-b-III tubulin antibody (ab14,545 Abcam, Cambridge, MA), an anti-IGF-IR antibody (#3027, Cell Signaling, Danvers, MA), or anti-phosphorylated IGF-IR (#3024, Cell Signaling) for 1 hr at room temperature. After washing with PBS three times, the cells were incubated with the secondary antibody (FITC-conjugated goat anti-mouse or anti-rabbit IgG) for 1 hr at room temperature. After three washes with PBS, the cells were further stained with 4′,6-diamidino-2-phenylindole (DAPI, for nuclear staining) for 5 min, examined under a fluorescence microscope, and photographed.

Western blot analysis

Cells were treated as described above in immunofluorescence staining. For time-course experiments, the incubation with PPP was extended to 3 and 24 hr in addition to the standard 1-hr incubation. The cells were then lysed in a lysis buffer containing 1% IGEPAL CA-630, 0.5% sodium deoxycholate, 0.1% SDS, aprotinin (10 µg/ ml), leupeptin (10 µg/ml), and PBS. Cell lysates containing 20 µg of protein were electrophoresed in SDS-PAGE and then transferred onto a PVDF membrane (Millipore Corp., Bedford, MA). The membrane was stained with Ponceau S to verify the integrity of the transferred proteins and to monitor the unbiased transfer of all protein samples. Detection of protein on the membrane was performed with the ECL kit (Amersham Life Sciences Inc., Arlington Heights, IL) using an anti-β-III tubulin antibody. The resulting images were analyzed with ChemiImager 4,000 (Alpha Innotech Corporation, San Leandro, CA) to determine the integrated density value (IDV) of each protein band. Before re-probing with an anti-β-actin antibody, the membrane was stripped in 62.5 mM Tris-HCl, pH 6.7, 2% SDS, 10 mM 2-mercaptoethanol at 561C for 30 min and then washed four times in $1 \times$ TBST.

Statistical analysis

Data were analyzed with Prism 4 (GraphPad Software Inc., San Diego, CA). A *t*-test was used to analyze the effects of IBMX and PPP on β-III-tubulin expression in ADSC. *p* value <0.05 was considered to be significant.

Results

Signaling pathway screening

We have shown previously that ADSC could be induced by IBMX to differentiate into neuron-like cells (Ning et al., 2006). In the present study, we used specific inhibitors of eight different signaling pathways to identify possible signaling mechanisms for IBMX-induced ADSC neuronal differentiation. We treated ADSC with IBMX in the presence or absence of each of these inhibitors for 1 hr, stained the cells with HE, and took pictures of the cells. From the photographs, a total of 1,000 cells in each treatment was scored as "+" for neuron-like morphology (condensed cell body with cellular processes) or "–" for non-neuron morphology (the original ADSC morphology). Representative photographs are shown in Figure 1. The scoring showed that 35% of the cells treated with IBMX+PPP assumed the neuron-like morphology, while approximately 95% of the cells treated with IBMX in the absence or in the presence of other inhibitors assumed the neuron-like morphology. Thus, PPP appeared to be the only inhibitor that could substantially suppress the IBMX-induced neuron-like differentiation of ADSC.

PPP suppresses IBMX-induced β-III-tubulin expression

The neuronal marker, β-III-tubulin, was highly inducible in IBMX-treated ADSC, as demonstrated by immunofluorescence staining (Fig. 2A) and Western blotting (Fig. 2B). Addition of PPP, however, suppressed this induction. PPP's suppressive effect was specific, because its solvent, DMSO, or the inhibitor of Wnt/Frizzled signaling, DKK-1, had no such suppressive effect (Fig. 2). For quantitative analysis of the suppressive effect of PPP and time-course study, three independent experiments were conducted for each time point at 1, 3, and 24 hr (duration of PPP treatment). The results show that PPP suppressed IBMX-induced β-III-tubulin expression by 43%, 88%, and 84% when used to treat the cells for 1, 3, and 24 hr, respectively (Fig. 3).

PPP suppresses IBMX-induced IGF-IR phosphorylation

Previous studies have shown that phosphorylation of tyrosine residue 1136 (Y1136) of IGF-IR is associated with IGF-IR activity, and PPP suppresses IGF-IR activity by inhibiting phosphorylation of Y1136, while sparing the other two tyrosine residues (Y1131 and Y1135) (Girnita et al., 2004; Vasilcanu et al., 2004). Therefore, we used an antibody (#3024, Cell Signaling) that reacts specifically with phosphorylated Y1136 to examine the phosphorylation status of IGF-IR in IBMX-treated ADSC in the absence and in the presence of PPP. Another antibody (#3027, Cell Signaling) that reacts with IGF-IR regardless of its phosphorylation status was also used, and it produced results (Fig. 4A) indicating similar expression levels of IGF-IR in both IBMX-(Induction) and IBMX+PPP-treated cells, despite the sharp difference in cell morphology. On the other hand, the antibody that reacts with phosphorylated Y1136 produced very different results in the expression level of phosphorylated IGF-IR in IBMX-(Induction) and IBMX+PPP-treated cells (Fig. 4B). Thus, while IBMX induced phosphorylation (activation) of IGF-IR, PPP suppressed this induction.

Discussion

ADSC have been shown to differentiate into neurons or neuron-like cells *in vitro* (Safford et al., 2002, 2004; Zuk et al., 2002; Ashjian et al., 2003; Tholpady et al., 2003; Yang et al., 2004; Case et al., 2005; Fujimura et al., 2005; Jack et al., 2005; Guilak et al., 2006; Ning et al., 2006) and *in vivo* (Kang et al., 2003, 2006). For *in vitro* neural differentiation, the experiments generally rely on treating ADSC with retinoic acid and cytokine cocktails (Case et al., 2005), butylated hydroxyanisole, DMSO (Safford et al., 2002; Zuk et al., 2002; Guilak et al., 2006), and agents that elevate intracellular cAMP levels (Ashjian et al., 2003; Fujimura et al., 2005; Ning et al., 2006). Cells treated with these agents can assume neuron-like morphology within hours, as reported previously by us and others (Zuk et al., 2002; Fujimura et al., 2005; Ning et al., 2006). Similar rapid neural differentiation has also been observed with BMSC treated with DMSO, and this observation had subsequently been interpreted as a manifestation of the toxic effects of DMSO. We have discussed this controversy in detail in our report (Ning et al., 2006).

Previously, we showed that IBMX could induce ADSC to undergo neuron-like differentiation (Ning et al., 2006). In the present study, we further investigated the molecular mechanism of this IBMX-induced ADSC neural differentiation. We first screened inhibitors of eight signaling pathways for their ability to prevent the neuron-like morphological changes of ADSC after IBMX treatment. While each of seven of the tested inhibitors prevented 5% of the IBMX-treated cells from assuming the neuronal morphology, PPP suppressed the morphological change in 65% of the IBMX-treated cells. The reason for the incomplete suppression by PPP is not clear, but the heterogeneous nature of ADSC suggests that certain cell types might be resistant to PPP treatment.

Although not entirely unexpected, we were surprised that only PPP was able to significantly suppress the morphological change of IBMX-treated ADSC. In particular, we had in fact anticipated another inhibitor, PD98059, to have such an effect due to its reported suppressive effect on forskolin-induced BMSC neural differentiation (Kim et al., 2005). However, despite being similar to forskolin as a cAMP-elevating agent, IBMX apparently induced ADSC neural differentiation through the IGF-I and not the ERK/MAPK pathway (target of PD98059). To confirm the neuronal effect of PPP, we showed that PPP was able to suppress the expression of neural marker β-III-tubulin in IBMX-treated ADSC (Fig. 2). Time-course study further showed that the suppressive effect of PPP on β-III-tubulin expression was stronger at 3 and 24 hr than at 1 hr post-treatment. Because PPP is known to inhibit the phosphorylation of IGF-IR (Vasilcanu et al., 2004), we also examined the phosphorylation status of IGF-IR in IBMX-treated ADSC in the absence and in the presence

of PPP. Specifically, it is known that PPP blocks the phosphorylation of tyrosine residue 1136 (Y1136), while sparing the other two tyrosine residues (Y1131 and Y1135) of IGF-IR (Vasilcanu et al., 2004); therefore, we used an antibody that reacts specifically with phosphorylated Y1136. The results showed that (1) IBMX-induced phosphorylation of IGF-IR at Y1136 in ADSC (Fig. 4A) and (2) PPP suppressed this induction (Fig. 4B). Thus, IBMX-induced ADSC neuronal differentiation is mediated by IGF-I signaling as it has been demonstrated that phosphorylation of IGF-IR at Y1136 is associated with IGF-IR activity (Girnita et al., 2004; Vasilcanu et al., 2004).

While the identification of IGF-I signaling as the underlying mechanism for ADSC neuronal differentiation is novel, it has been well documented that the IGF system plays important roles in the development of the nervous system (Russo et al., 2005). *In vitro* studies have demonstrated that the IGF system promotes differentiation and proliferation of neurons and sustains their survival by preventing apoptosis. *In vivo* studies of transgenic mice overexpressing components of the IGF system or mice with disruptions of the same genes have clearly shown that the IGF system plays key roles in brain development (Russo et al., 2005). For example, IGF-IR knock-out mice have reduced brain size, CNS hypomyelination, and loss of hippocampal granule and striatal parvalbumin-containing neurons (Beck et al., 1995). On the other hand, transgenic mice overexpressing IGF-I had fewer apoptotic neurons during early postnatal development of the cerebral cortex and this has led to a persistent increase in total neuron number even in the adult animal (Hodge et al., 2007).

In the adult brain, the IGF system continues to influence neurogenesis through its effects on the adult neural progenitor cells (Brooker et al., 2000; Anderson et al., 2002; McCurdy et al., 2005). Thus, while IGF-I signaling is undoubtedly important for the development of the nervous system and for the continuing neuro-genesis of adult neural progenitor cells, the findings in the present study provide the first piece of evidence that IGF-I signaling also mediates the neurogenesis of cells of non-neural origin. Whether IGF itself has an effect on ADSC's neuronal differentiation is currently being investigated in our laboratory. Our preliminary studies with rat models of neurogenic erectile dysfunction and urinary incontinence did show that ADSC were able to accelerate recovery of neural function.

Acknowledgments

References

Anderson MF, Aberg MA, Nilsson M, Eriksson PS. Insulin-like growth factor-I and neurogenesis in the adult mammalian brain. Brain Res Dev Brain Res 2002;134:115–122.

Ashjian PH, Elbarbary AS, Edmonds B, DeUgarte D, Zhu M, Zuk PA, Lorenz HP, Benhaim P, Hedrick MH. In vitro differentiation of human processed lipoaspirate cells into early neural progenitors. Plast Reconstr Surg 2003;111:1922–1931. [PubMed: 12711954]

Beck KD, Powell-Braxton L, Widmer HR, Valverde J, Hefti F. Igf1 gene disruption results in reduced brain size, CNS hypomyelination, and loss of hippocampal granule and striatal parvalbumin-containing neurons. Neuron 1995;14:717–730. [PubMed: 7718235]

Brooker GJ, Kalloniatis M, Russo VC, Murphy M, Werther GA, Bartlett PF. Endogenous IGF-1 regulates the neuronal differentiation of adult stem cells. J Neurosci Res 2000;59:332–341. [PubMed: 10679768]

Case J, Horvath TL, Howell JC, Yoder MC, March KL, Srour EF. Clonal multilineage differentiation of murine common pluripotent stem cells isolated from skeletal muscle and adipose stromal cells. Ann NY Acad Sci 2005;1044:183–200. [PubMed: 15958712]

De Ugarte DA, Morizono K, Elbarbary A, Alfonso Z, Zuk PA, Zhu M, Dragoo JL, Ashjian P, Thomas B, Benhaim P, Chen I, Fraser J, Hedrick MH. Comparison of multi-lineage cells from human adipose tissue and bone marrow. Cells Tissues Organs 2003;174:101–109. [PubMed: 12835573]

Dicker A, Le Blanc K, Astrom G, van Harmelen V, Gotherstrom C, Blomqvist L, Arner P, Ryden M. Functional studies of mesenchymal stem cells derived from adult human adipose tissue. Exp Cell Res 2005;308:283–290. [PubMed: 15925364]

Fujimura J, Ogawa R, Mizuno H, Fukunaga Y, Suzuki H. Neural differentiation of adipose-derived stem cells isolated from GFP transgenic mice. Biochem Biophys Res Commun 2005;333:116–121. [PubMed: 15939405]

Girnita A, Girnita L, del Prete F, Bartolazzi A, Larsson O, Axelson M. Cyclolignans as inhibitors of the insulin-like growth factor-1 receptor and malignant cell growth. Cancer Res 2004;64:236–242. [PubMed: 14729630]

Gronthos S, Franklin DM, Leddy HA, Robey PG, Storms RW, Gimble JM. Surface protein characterization of human adipose tissue-derived stromal cells. J Cell Physiol 2001;189:54–63. [PubMed: 11573204]

Guilak F, Lott KE, Awad HA, Cao Q, Hicok KC, Fermor B, Gimble JM. Clonal analysis of the differentiation potential of human adipose-derived adult stem cells. J Cell Physiol 2006;206:229–237. [PubMed: 16021633]

Hodge RD, D'Ercole AJ, O'Kusky JR. Insulin-like growth factor-I (IGF-I) inhibits neuronal apoptosis in the developing cerebral cortex in vivo. Int J Dev Neurosci 2007;25:233–241. [PubMed: 17459648]

Housman TS, Lawrence N, Mellen BG, George MN, Filippo JS, Cerveny KA, DeMarco M, Feldman SR, Fleischer AB. The safety of liposuction: results of a national survey. Dermatol Surg 2002;28:971–978. [PubMed: 12460288]

Jack GS, Almeida FG, Zhang R, Alfonso ZC, Zuk PA, Rodriguez LV. Processed lipoaspirate cells for tissue engineering of the lower urinary tract: implications for the treatment of stress urinary incontinence and bladder reconstruction. J Urol 2005;174:2041–2045. [PubMed: 16217390]

Kang SK, Lee DH, Bae YC, Kim HK, Baik SY, Jung JS. Improvement of neurological deficits by intracerebral transplantation of human adipose tissue-derived stromal cells after cerebral ischemia in rats. Exp Neurol 2003;183:355–366. [PubMed: 14552877]

Kang SK, Shin MJ, Jung JS, Kim YG, Kim CH. Autologous adipose tissue-derived stromal cells for treatment of spinal cord injury. Stem Cells Dev 2006;15:583–594. [PubMed: 16978061]

Kim SS, Choi JM, Kim JW, Ham DS, Ghil SH, Kim MK, Kim-Kwon Y, Hong SY, Ahn SC, Kim SU, Lee YD, Suh-Kim H. cAMP induces neuronal differentiation of mesenchymal stem cells via activation of extracellular signal-regulated kinase/MAPK. Neuroreport 2005;16:1357–1361. [PubMed: 16056139]

Laping NJ, Grygielko E, Mathur A, Butter S, Bomberger J, Tweed C, Martin W, Fornwald J, Lehr R, Harling J, Gaster L, Callahan JF, Olson BA. Inhibition of transforming growth factor (TGF)-beta1-induced extracellular matrix with a novel inhibitor of the TGF-beta type I receptor kinase activity: SB-431542. Mol Pharmacol 2002;62:58–64. [PubMed: 12065755]

Lee RH, Kim B, Choi I, Kim H, Choi HS, Suh K, Bae YC, Jung JS. Characterization and expression analysis of mesenchymal stem cells from human bone marrow and adipose tissue. Cell Physiol Biochem 2004;14:311–324. [PubMed: 15319535]

Lin G, Bella AJ, Lue TF, Lin CS. Brain-derived neurotrophic factor (BDNF) acts primarily via the JAK/STAT pathway to promote neurite growth in the major pelvic ganglion of the rat: part 2. J Sex Med 2006;3:821–827. discussion 828–829. [PubMed: 16942527]

Liu TM, Martina M, Hutmacher DW, Hui JH, Lee EH, Lim B. Identification of common pathways mediating differentiation of bone marrow- and adipose tissue-derived human mesenchymal stem cells into three mesenchymal lineages. Stem Cells 2007;25:750–760. [PubMed: 17095706]

Mao B, Wu W, Li Y, Hoppe D, Stannek P, Glinka A, Niehrs C. LDL-receptor-related protein 6 is a receptor for Dickkopf proteins. Nature 2001;411:321–325. [PubMed: 11357136]

McCurdy RD, Feron F, McGrath JJ, Mackay-Sim A. Regulation of adult olfactory neurogenesis by insulin-like growth factor-I. Eur J Neurosci 2005;22:1581–1588. [PubMed: 16197498]

Ning H, Lin G, Lue TF, Lin CS. Neuron-like differentiation of adipose tissue-derived stromal cells and vascular smooth muscle cells. Differentiation 2006;74:510–518. [PubMed: 17177848]

Russo VC, Schutt BS, Andaloro E, Ymer SI, Hoeflich A, Ranke MB, Bach LA, Werther GA. Insulin-like growth factor binding protein-2 binding to extracellular matrix plays a critical role in neuroblastoma cell proliferation, migration, and invasion. Endocrinology 2005;146:4445–4455. [PubMed: 15994346]

Safford KM, Hicok KC, Safford SD, Halvorsen YD, Wilkison WO, Gimble JM, Rice HE. Neurogenic differentiation of murine and human adipose-derived stromal cells. Biochem Biophys Res Commun 2002;294:371–379. [PubMed: 12051722]

Safford KM, Safford SD, Gimble JM, Shetty AK, Rice HE. Characterization of neuronal/glial differentiation of murine adipose-derived adult stromal cells. Exp Neurol 2004;187:319–328. [PubMed: 15144858]

Strem BM, Hicok KC, Zhu M, Wulur I, Alfonso Z, Schreiber RE, Fraser JK, Hedrick MH. Multipotential differentiation of adipose tissue-derived stem cells. Keio J Med 2005;54:132–141. [PubMed: 16237275]

Tholpady SS, Katz AJ, Ogle RC. Mesenchymal stem cells from rat visceral fat exhibit multipotential differentiation in vitro. Anat Rec A Discov Mol Cell Evol Biol 2003;272:398–402. [PubMed: 12704697]

Vasilcanu D, Girnita A, Girnita L, Vasilcanu R, Axelson M, Larsson O. The cyclolignan PPP induces activation loop-specific inhibition of tyrosine phosphorylation of the insulin-like growth factor-1 receptor. Link to the phosphatidyl inositol-3 kinase/Akt apoptotic pathway. Oncogene 2004;23:7854–7862. [PubMed: 15334055]

Wagner W, Wein F, Seckinger A, Frankhauser M, Wirkner U, Krause U, Blake J, Schwager C, Eckstein V, Ansorge W, Ho AD. Comparative characteristics of mesenchymal stem cells from human bone marrow, adipose tissue, and umbilical cord blood. Exp Hematol 2005;33:1402–1416. [PubMed: 16263424]

Yang LY, Liu XM, Sun B, Hui GZ, Fei J, Guo LH. Adipose tissue-derived stromal cells express neuronal phenotypes. Chin Med J (England) 2004;117:425–429. [PubMed: 15043785]

Yoshimura H, Muneta T, Nimura A, Yokoyama A, Koga H, Sekiya I. Comparison of rat mesenchymal stem cells derived from bone marrow, synovium, periosteum, adipose tissue, and muscle. Cell Tissue Res 2007;327:449–462. [PubMed: 17053900]

Zuk PA, Zhu M, Ashjian P, De Ugarte DA, Huang JI, Mizuno H, Alfonso ZC, Fraser JK, Benhaim P, Hedrick MH. Human adipose tissue is a source of multipotent stem cells. Mol Biol Cell 2002;13:4279–4295. [PubMed: 12475952]

Zuk PA, Zhu M, Mizuno H, Huang J, Futrell JW, Katz AJ, Benhaim P, Lorenz HP, Hedrick MH. Multilineage cells from human adipose tissue: implications for cell-based therapies. Tissue Eng 2001;7:211–228. [PubMed: 11304456]
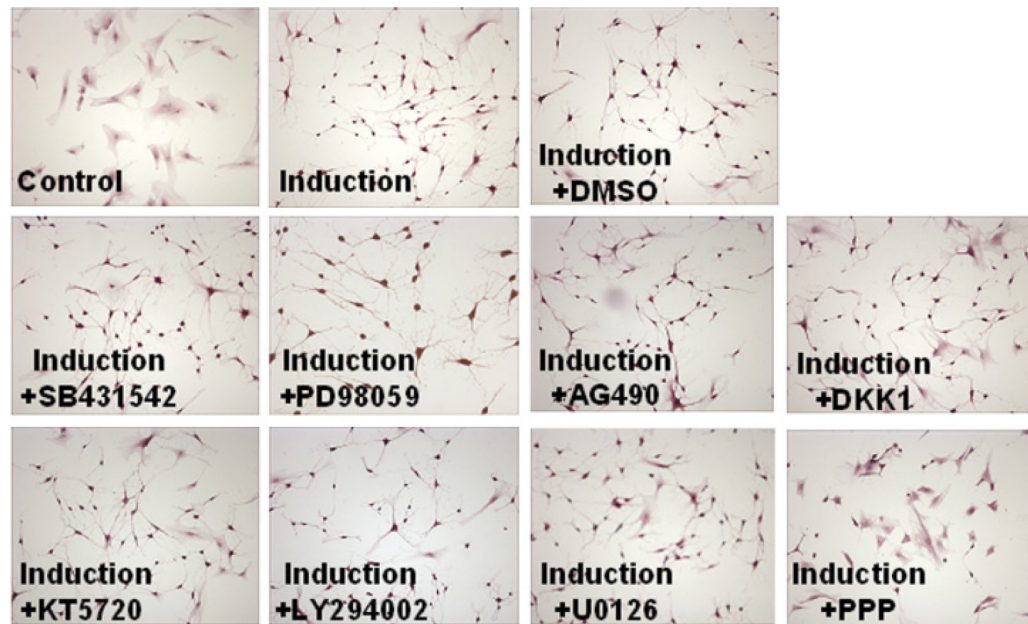
Fig. 1.
Signaling pathway screening. Adipose tissue-derived stem cells were seeded into six-well plates at 40%–60% confluence in Dubelco's modified Eagle's medium. The next day, each inhibitor was added at an effective concentration (Table 1). One hour later, the cells were washed three times with phosphate-buffered saline and treated with 500 mM isobutylmethylxanthine (IBMX) in the presence or in the absence of the same inhibitor for another hour. The cells were then processed for HE staining, visualized under a microscope, and photographed. Cells in "control" received neither IBMX nor any inhibitor. Cells in "induction" received only IBMX. Cells in "induction+DMSO" received IBMX and DMSO (solvent for all chemical inhibitors). Cells in each of the other panels received IBMX and the indicated inhibitor. Original magnification was $\times$ 200.
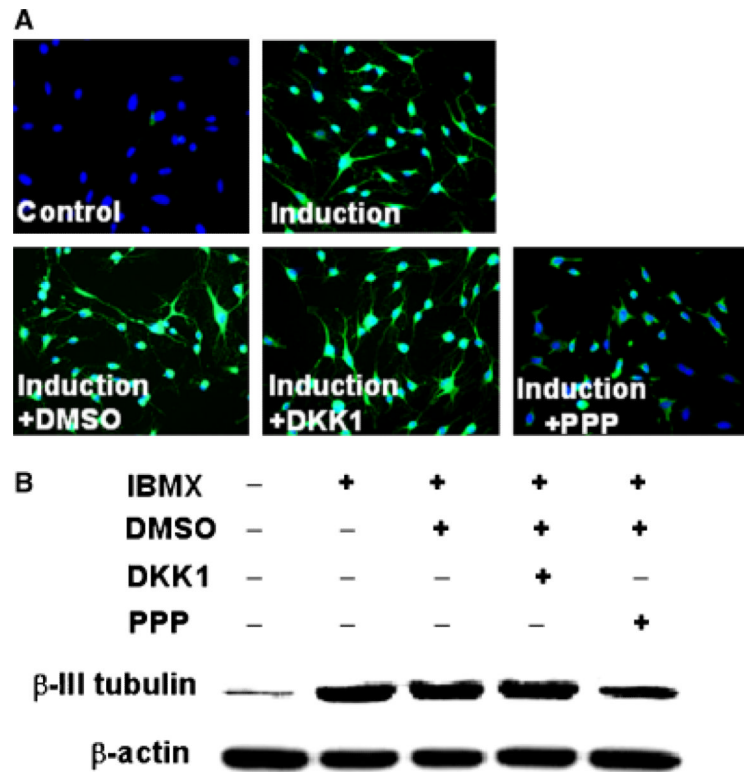
Fig. 2.
Effects of isobutylmethylxanthine (IBMX) and PPP on β-III-tubulin expression. (**A**)
Adipose tissue-derived stem cells (ADSC) were treated with IBMX and DKK-1 (inhibitor of
Wnt/Frizzled pathway) or PPP, as described in Figure 1. The cells were then processed for
immunofluorescence staining with an anti-β-III-tubulin antibody and with diamidino-2-
phenylindole. Green fluorescence indicates β-III-tubulin expression; blue fluorescence
indicates cell nucleus. Original magnification was × 200. (**B**) ADSC were treated as in (A)
and then processed for Western blotting with an anti-β-III-tubulin antibody and an anti-β-
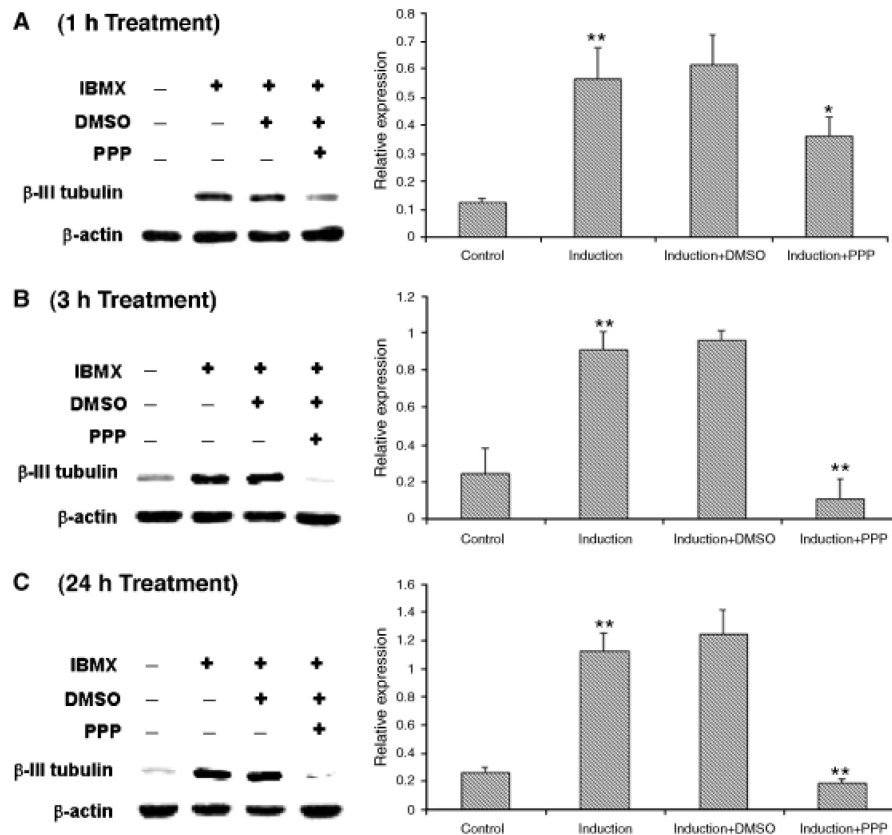actin antibody.

Fig. 3.
Time course of the effects of isobutylmethylxanthine (IBMX) and PPP on β-III-tubulin
expression. Adipose tissue-derived stem cells were treated with IBMX and PPP, as
described in Figure 1, and for additional time points at 3 and 24 hr. The cells were then
processed for Western blotting with an anti-β-III-tubulin antibody and an anti-β-actin
antibody. The resulting radiographs were analyzed by densitometry, and the data by Prism 4
software. For each time point (**A**, 1 hr; **B**, 3 hr; **C**, 24 hr), a representative radiograph is
shown on the left and the statistical analysis data on the right. "Relative expression" is the
ratio of β-III-tubulin versus β-actin expression. Each bar represents the average of 3
independent experiments. The asterisks above the second bar (induction) indicate significant
difference (p<0.01) between "induction" and "control." The asterisks above the fourth bar
(induction+PPP) indicate significant difference (*p<0.05; **p<0.01) between "induction
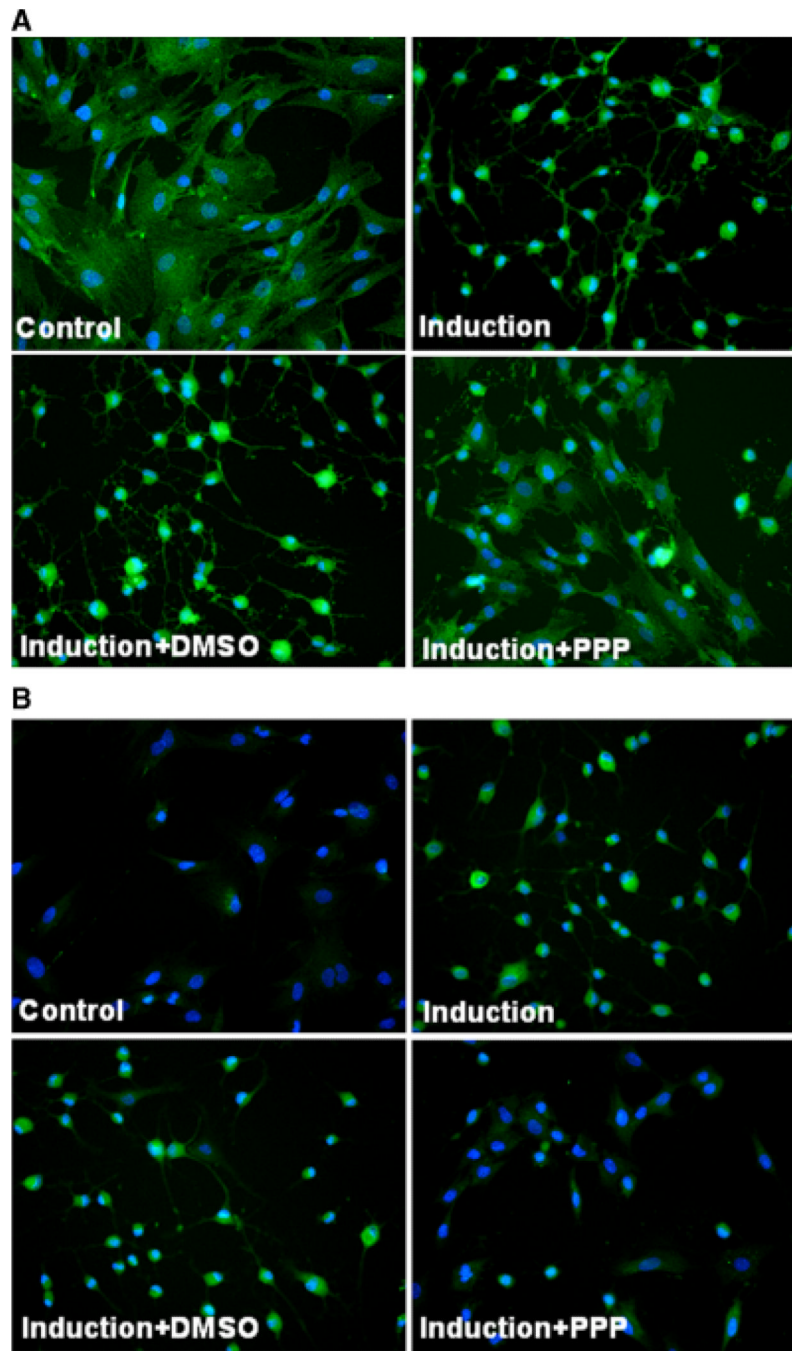+PPP" and "induction+DMSO."

Fig. 4.
Effects of isobutylmethylxanthine (IBMX) and PPP on expression and phosphorylation of Insulin growth factor (IGF)-IR. (**A**) Adipose tissue-derived stem cells were treated with IBMX and PPP, as described in Figure 1. The cells were then processed for immunofluorescence staining with anti-IGF-IR antibody, anti-phospho-IGF-IR antibody, and diamidino-2-phenylindole. Green fluorescence indicates IGF-IR expression (A) or phospho-IGF-IR expression (**B**); blue fluorescence indicates cell nucleus. Original magnification was × 200.

Table 1

Specific inhibitors of signaling pathways

Inhibitor	Target pathway	Concentration	Supplier
AG490	JAK/STAT	50 μM	
KT5720	PKA	800 nM	
LY294002	PI3-K	50 μM	EMD Biosciences, La Jolla, CA
U0126	MEK	25 μM	
PPP	IGF-I	2.5 μM	
DKK-1	Wnt/Frizzled	100 ng/ml	R&D system, Minneapolis, MN
PD98059	ERK/MAPK	5 μM	Sigma-Aldrich
SB431542	TGF-β	1 μM	Corporation

IGF, Insulin growth factor.